REPORT R-568 MAY, 1972 UILU-ENG 72-2229

CSL COORDINATED SCIENCE LABORATORY

# FIELD EVAPORATION: MODEL AND EXPERIMENT

MARIAN VESELY
GERT EHRLICH

UNIVERSITY OF ILLINOIS - URBANA, ILLINOIS

UILU-ENG 72-2229

# FIELD EVAPORATION: MODEL AND EXPERIMENT

by

Marian Vesely and Gert Ehrlich

This work was supported by the Air Force Office of Scientific Research (AFSC), USAF, under Grant AFOSR 69-1671 and 72-2210.

# FIELD EVAPORATION: MODEL AND EXPERIMENT

Marian Vesely and Gert Ehrlich
Coordinated Science Laboratory and Department of Metallurgy
University of Illinois at Urbana-Champaign
Urbana, Illinois

## Abstract

The ability of the image potential and charge exchange models to describe the evaporation of metals in a high electric field is examined. At present only the field dependence of the evaporation rate can be compared with the predictions of the two models. An analysis of the available experiments on the evaporation of tungsten atoms from kink sites, as well as from sites on top of the (110), suggests that the image potential model gives the most satisfactory representation of the data. The difference $\alpha$ between the polarizability of a neutral surface atom and an ion, which is obtained from a least-squares analysis, is found to differ little from one site to the next. For tungsten at a kink site $\alpha = 4.80 \pm .03$ $\text{Å}^3$; for an adatom on the (110), $\alpha = 5.24 \pm .04$ $\text{Å}^3$.

# FIELD EVAPORATION: MODEL AND EXPERIMENT[†]

Marian Vesely and Gert Ehrlich
Coordinated Science Laboratory and Department of Metallurgy
University of Illinois at Urbana-Champaign
Urbana, Illinois

Field evaporation, the removal of surface atoms by the application of a high electric field, is becoming increasingly important in the study of crystal interfaces. Potentially its most significant application lies in determining the binding energy of single surface atoms on sites of different atomic configuration;[1,2] this is a parameter of great interest that has not proved accessible to any other technique. Field evaporation is also basic to the general utilization of the field ion microscope, as well as to the understanding and interpretation of the newest of the projection microscopes, Müller's Atom Probe.[3]

Despite this wide range of applications, the mechanism whereby atoms are removed in a high field is not well understood and the application of this promising technique to important problems rests on uncertain foundations. Two different models have been proposed in the past to account for field evaporation. As yet their predictions have not been compared critically with experiment to assess the validity of the different views. This will be our modest aim here.

## THE MECHANISM OF FIELD EVAPORATION

### Image Potential Model

In his pioneering studies of the field ion microscope, E.W. Müller[3,4]

[†]Supported by the Air Force Office of Scientific Research (AFSC), USAF, under Grant AFOSR 69-1671 and 72-2210.

viewed field evaporation as the escape of a metal ion, of charge n, over a barrier resulting from the superposition of two effects: the potential -Fnex, created by the applied field F at a distance x from the image plane, and the image potential $-\frac{(ne)^2}{4x}$ which attracts the ion to the surface. At the Schottky saddle, as the maximum in the potential is known this superposition reduces the energy of the ion by an amount $(ne)^{3/2}F^{1/2}$ below the zero field value. If this reduction is comparable to $\chi_o^{+n}$, the energy to remove an ion from the surface in the absence of a field, then evaporation can take place even at extremely low temperatures.

This model has since been refined and is illustrated in Fig. 1 with schematic curves for the potential energy of the atomic and ionic species in their dependence upon the distance x. The assumptions made have been extensively analyzed; they are briefly:

1. Interactions between ion and crystal surface can be quantitatively described by an image potential.

It appears from several recent studies that the classical image potential is a serviceable approximation to the behavior of an ion at a real metal, provided x is taken as a sum of the distance from the ion core to the classical image plane, plus the screening length of the metal $\delta$.[5,6] The latter can be approximated by the Thomas-Fermi screening parameter $1/\lambda$, with a correction involving the Fermi wave number $k_F$, and is of the form

$$\delta = \lambda^{-1} + \pi(4k_F)^{-1}$$

At a real metal we must also account for field penetration in calculating the potential energy of an ion in the electric field. In the

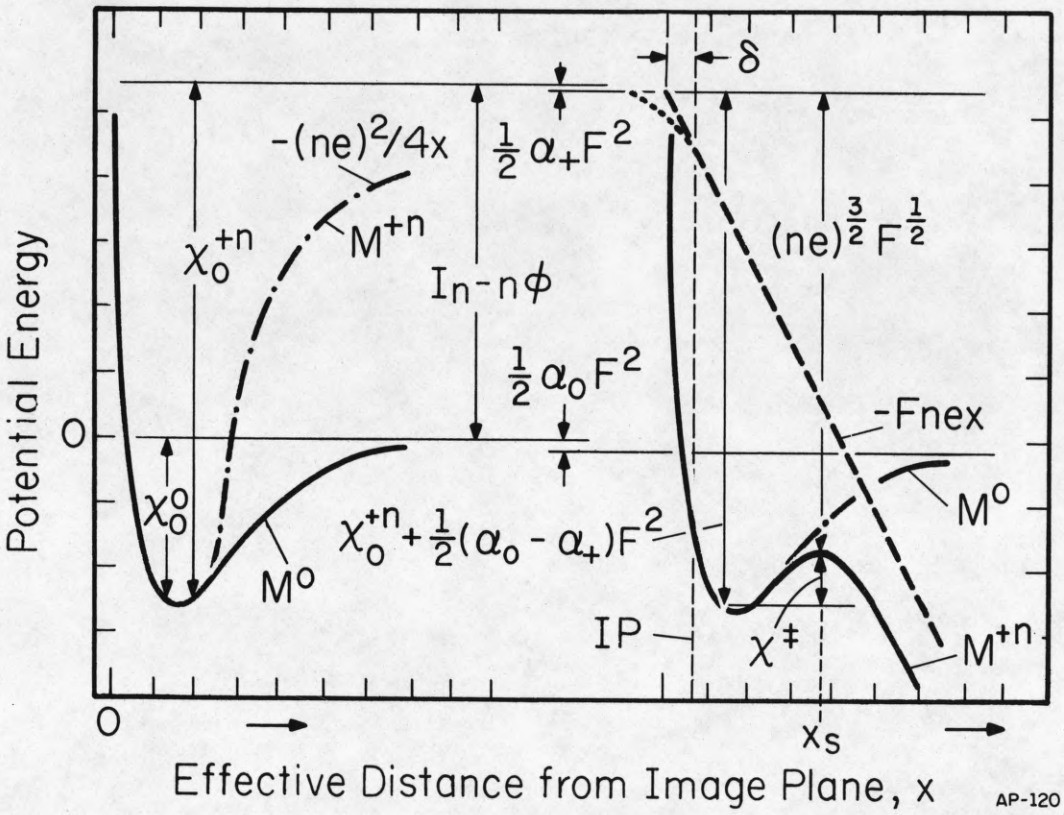


Fig. 1 Schematic potential diagram for the field evaporation of a metal according to the image potential model. $M^o$ = neutral metal atom; $M^{+n}$ = metal ion with charge +n. $\chi^\ddagger$ = activation energy for field evaporation; IP = image plane; $\delta$ = screening length; $x_s$ = location of Schottky hump.

expression -Fnex, the distance x must again include the screening length $\delta$. The energy of the ion at the Schottky saddle therefore remains unchanged.[7,8,9] In this description no account is taken of any repulsive effects as the ion core approaches within atomic distances of the surface. The validity of this neglect is doubtful.[10]

2. In the applied field the neutral surface atom loses one or more electron prior to reaching $x_s$, the location of the Schottky maximum in the ionic curve.

This will be true only if the ionic curve falls below the atomic potential before the Schottky saddle is reached. A direct assessment of this assumption demands a detailed knowledge of the interaction of atoms and ions with the surface. As such information is presently not available, an *á priori* decision is not possible.

3. The interaction of the field with the neutral atom in its ground state is represented as a polarization energy, $\frac{1}{2}\alpha_o F^2$, where $\alpha_o$ is the polarizability of the surface atom. A similar but smaller correction involving the polarizability $\alpha_+$ is inserted for the energy of the ion.

Higher order interactions of the form $\frac{1}{24}\gamma F^4$, involving the hyperpolarizability $\gamma$, may have to be invoked for a more adequate representation of these interactions.[11] The possibility of such additional terms must be kept in mind throughout, and will be explicitly considered in the actual analysis of experimental data.

Provided desorption occurs at temperatures high enough to insure that escape over the barrier, rather than tunnelling through it, is the primary mechanism, then the rate of field evaporation is given by

$$k_E = \nu \exp - \frac{\chi^{\ddagger}}{kT} . \qquad (1)$$

Here $\nu$ is a frequency factor, and $\chi^{\ddagger}$ the height of the barrier measured from the ground state of the surface atom in the field. Under the assumptions outlined, the height of the barrier is just the difference between two levels: the Schottky saddle, modified by ion polarization, located at an energy $(ne)^{3/2}F^{1/2} + \frac{1}{2}\alpha_+F^2$ below the vacuum level of the free ion, and the ground state of the neutral atom, $\chi_o^{+n} + \frac{1}{2}\alpha_oF^2$ below the free ion. The barrier $\chi^{\ddagger}$ is thus given as

$$\chi^{\ddagger} = \chi_o^{+n} + \frac{1}{2}(\alpha_0-\alpha_+)F^2 - (ne)^{3/2}F^{1/2}. \qquad (2)$$

We will define an effective polarizability $\alpha \equiv \alpha_o-\alpha_+$ to simplify the presentation. The energy to create a free ion in the absence of the field, $\chi_o^{+n}$, is simply related to $\chi_o^o$, the energy of vaporization (at $T = 0^oK$) of the neutral atom. This is the usual quantity of interest. Provided we know the work function $\phi$ of the surface, as well as $I_n$, the energy to create an ion of charge $+n$ in field free space starting from the neutral atom, then $\chi_o^o$ is determined by

$$\chi_o^{+n} = \chi_o^o + I_n - n\phi. \qquad (3)$$

The desorption barrier for the image model can now be written in the usual form

$$\chi^{\ddagger} = \chi_o^o + I_n - n\phi - (ne)^{3/2}F^{1/2} + \frac{1}{2}\alpha F^2. \qquad (4)$$

This expression rests entirely on our assumed knowledge of the potential governing the behavior of the ion. It gives the complete form of the barrier to desorption, subject only to the assumptions already listed. The work function, as well as the ionization potential, should be recognized as zero field values, which enter only in relating the desorption energy of a neutral to the desorption energy of the ion. It is the latter quantity which is directly accessible to experiment.

Charge Exchange

In the alternative model of field evaporation, the process of charge exchange in which the ion is created, is postulated as the limiting step. This picture was first proposed for the desorption of electronegative gases in a high field.[7] However, it would also be the more appropriate model[12] for a metal, if the Schottky saddle for the ion lies closer to the surface than the intersection of the atomic with the ionic potential at $x_c$. In view of our lack of information about the actual potentials, an assignment of the crossing point in any real system is at present not possible.

Potential curves appropriate for the charge exchange model are displayed in Fig. 2. The highest point on the potential surface is now at the intersection of the atomic and ionic curves, located at a distance $x_c$ from the image plane (corrected for field penetration). At $x_c$ the energy of the ion, or equivalently the atom, relative to that of the free ion is

$$-\frac{(ne)^2}{4x_c} - Fnex_c - \frac{1}{2}\alpha_+ F^2 - \Gamma,$$

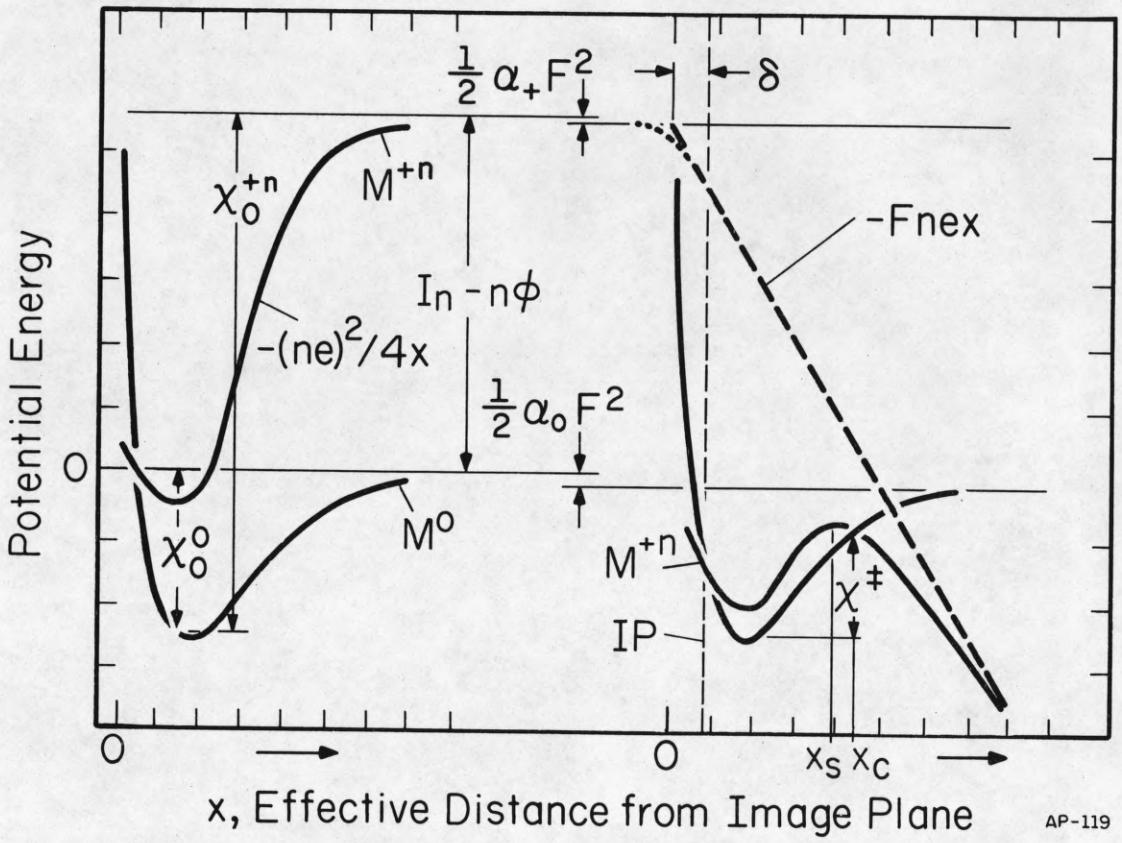


Fig. 2 Potential curves for charge exchange model of field evaporation. $x_c$ = point of intersection for atomic and ionic curves. The half-width $\Gamma$ due to interaction between the curves is not indicated.

where $\Gamma$ is the half-width of the ionic level broadened by interaction with the atomic curve (an effect not explicitly indicated in Fig. 2.). The energy of the ground state, relative to that of the free ion, is

$$-\chi_o^{+n} - \frac{1}{2}\alpha_o F^2 \ .$$

The difference between these two quantities gives the barrier for the removal of an ion with charge n as

$$\chi^{\ddagger} = \chi_o^{+n} - \frac{(ne)^2}{4x_c} - \Gamma - Fnex_c + \frac{1}{2}\alpha F^2. \qquad (5)$$

Making use of Eq. (3) to relate the desorption energy of the ion to that of the atom, we can finally write

$$\chi^{\ddagger} = \chi_o^{o} + I_n - n\phi - \frac{(ne)^2}{4x_c} - \Gamma - Fnex_c + \frac{1}{2}\alpha F^2. \qquad (6)$$

Except for the difference in the limiting step, the assumptions underlying this model are precisely the same as for the image force picture of desorption. However, a prediction of the desorption barrier now requires a knowledge of both the atomic and ionic curves, as it is their intersection which dictates the crossing point $x_c$. Since this is lacking, a decision on the merits of the two models must rest entirely on their relative ability to describe experiment.

## TESTS OF DESORPTION MODELS

The image potential model has proved quite successful in predicting the fields required for the evaporation of a whole series of metals at low

temperatures.[3] However, a decisive test of its applicability is not possible in this way. Formally, the evaporation field at absolute zero can be obtained from Eq. (4) by setting the barrier height to zero. However, the effective polarizability $(\alpha_o - \alpha_+) \equiv \alpha$ that enters into this equation is not known through independent measurements. Furthermore, for many of the transition elements, especially in the sixth period, the higher ionization potentials have not been determined.[13]

A different approach toward testing the validity of field evaporation models was initiated by Brandon;[14] he suggested and carried out measurements of both the temperature and field dependence of the evaporation rate. It is the latter that will concern us, as measurements of the evaporation of tungsten over a fair range of fields have recently become available in a series of elegant experiments.[11,12]

For the image model, the field dependence of evaporation can be explored most simply by recasting Eq. 1 and 2 in the form

$$\ln k_E - \frac{(ne)^{3/2} F^{1/2}}{kT} = \ln \nu - \frac{\chi_o^{+n}}{kT} - \frac{1}{2}\frac{\alpha F^2}{kT}. \qquad (7)$$

A plot of $\ln k_E - \frac{(ne)^{3/2} F^{1/2}}{kT}$ against $F^2$ should yield a straight line with a slope of $-\frac{1}{2}\alpha/kT$. It has been noted that absolute values of the rate constant for field evaporation, $k_E$, are available only for adsorbed atoms.[11] For these, $\chi_o^{+n}$, the energy for desorbing an ion, which enters the intercept, is not known from independent measurements.[1] The adequacy of the image model as a representation of field evaporation can therefore be judged only by the ability of Eq. (7) to portray the variation with field. This equation requires a knowledge of the charge state of the ion created in the

evaporation process. On the image model it is predicted that doubly charged ions should be formed for most of the refractory transition elements,[15] a prediction verified in experiments on W[16] and Ni[17] some time ago. However, in more recent studies with the Atom Probe, Müller and co-workers have discovered a whole range of ions.[18] The mechanism of their formation is not yet understood, and n must therefore be considered as an additional unspecified parameter.

For evaporation involving charge exchange as the limiting step, the rate equation is most conveniently expressed in the form

$$\ln k_E = \ln \nu - \frac{1}{kT}\left[\chi_o^{+n} - \frac{(ne)^2}{4x_c} - \Gamma\right] + \frac{Fnex_c}{kT} - \frac{1}{2}\frac{\alpha F^2}{kT} \quad . \tag{8}$$

The logarithm of the rate constant should now be best represented by a second order polynomial in the field provided the crossing point $x_c$ does not depend sensitively upon F.[3] Quantitative information on $x_c$ is not available, and the first order field coefficient serves as just another adjustable parameter. In this model the polarizability $\alpha$ is therefore derived from the coefficient of the second order term without any knowledge of n, the charge of the ion. This constitutes an important difference from Eq. (7) governing the image potential model; there, except for n, the coefficient of the term in $F^{1/2}$ is specified quantitatively.

Just as above, there is not enough information to independently validate estimates of the coefficients derived in this way from experiment; we can at best predict their rough magnitude from simple physical considerations. At present, the difference in the field dependence of Eqs. (7)

and (8) affords the only hope of establishing the relative validity of the two models for the evaporation process.

## COMPARISON WITH EXPERIMENT

### Data Analysis

A sample of the quantitative data available on field evaporation of tungsten is given in Fig. 3, showing the kinetics of single atom removal from the (110) plane. The values of log $k_E$ as a function of the field were obtained from graphs kindly supplied by Dr. Tsong, using an Auto-trol 3400 Digitizer. To test the adequacy of the charge exchange model against the image potential picture, the data on log $k_E$ were fitted either to a second order polynomial in F,

$$\log k_E = B(0) + B(1)F + B(2)F^2$$

as in Eq. (8), or else to a relation of the form of Eq. (7), in which

$$\log k_E - \frac{(ne)^{3/2}F^{1/2}}{2.303\ kT} = B(0) + B(2)F^2.$$

The results of the least squares analysis[19] of these two possible regression curves, with equal weight assigned to each experimental value of log $k_E$, are summarized in Table I. Four different data sets were examined: two for the evaporation of atoms from kink sites at steps in the (110) plane of tungsten, and two for the evaporation of single tungsten adatoms placed on top of the (110). The designation of the data set includes, where necessary, the figure

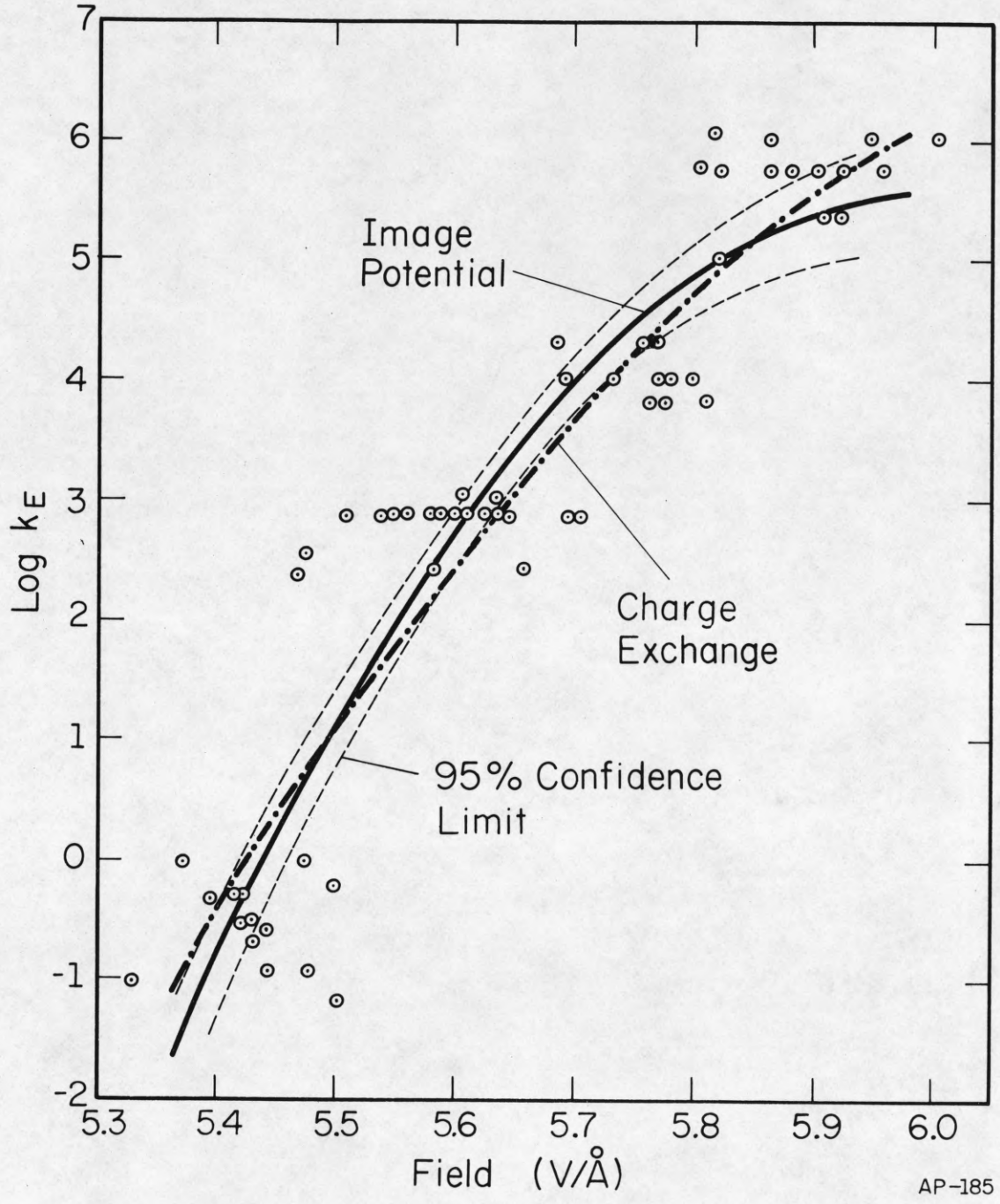


Fig. 3 Rate of field evaporation for W adatoms from W(110). Charge exchange curve - data fitted by Eq.(8); Image potential - data fitted by Eq.(7), with n = +2. Experimental data-set TT10, Reference 11.

Table I

SECOND ORDER ANALYSIS OF FIELD EVAPORATION

| Atom | Ref. | Model | n | σ | Polynomial Coefficients B(0) | t-t | B(1) | t-t | B(2) | t-t | $x_c$, Å | α, Å$^3$ |
|---|---|---|---|---|---|---|---|---|---|---|---|---|
| Kink | TM | Charge X | 2 | .81 | -533.8 | $8\cdot10^{-3}$ | 165.0 | $1\cdot10^{-2}$ | -12.59 | $1.8\cdot10^{-2}$ | $1.27 \pm .45$[a] | $5.56 \pm 2.15$[b] |
| | | | 3 | | | | | | | | $.84 \pm .30$ | |
| | | Image | 2 | .80 | -1324.5 | $<10^{-5}$ | | | -10.71 | $<10^{-5}$ | | $4.73 \pm .03$ |
| | | | 3 | 1.07 | -2403.2 | $<10^{-5}$ | | | -20.56 | $<10^{-5}$ | | $9.09 \pm .04$ |
| | TT7 | Charge X | 2 | .07 | -438.0 | $3\cdot10^{-3}$ | 135.6 | $3\cdot10^{-3}$ | -10.37 | $4\cdot10^{-3}$ | $1.04 \pm .06$ | $4.58 \pm .28$ |
| | | | 3 | | | | | | | | $.69 \pm .04$ | |
| | | Image | 2 | .41 | 1318.4 | $<10^{-5}$ | | | -10.89 | $<10^{-5}$ | | $4.81 \pm .03$ |
| | | | 3 | 1.35 | -2399.8 | $<10^{-5}$ | | | -20.66 | $<10^{-5}$ | | $9.13 \pm .09$ |
| Adatom on (110) | TT9 | Charge X | 2 | 1.10 | -131 | .25 | 36 | .36 | -2.2 | .51 | $.28 \pm .30$ | $0.99 \pm 1.51$ |
| | | | 3 | | | | | | | | $.18 \pm .20$ | |
| | | Image | 2 | 1.37 | -1284.6 | $<10^{-5}$ | | | -11.77 | $<10^{-5}$ | | $5.20 \pm .04$ |
| | | | 3 | 1.98 | -2337.5 | $<10^{-5}$ | | | -22.36 | $<10^{-5}$ | | $9.88 \pm .05$ |
| | TT10 | Charge X | 2 | .84 | -385 | $2\cdot10^{-3}$ | 125 | $3\cdot10^{-3}$ | -10.02 | $8\cdot10^{-3}$ | $.96 \pm .31$ | $4.43 \pm 1.60$ |
| | | | 3 | | | | | | | | $.64 \pm .21$ | |
| | | Image | 2 | .87 | -1278.4 | $<10^{-5}$ | | | -11.92 | $<10^{-5}$ | | $5.27 \pm .03$ |
| | | | 3 | 1.13 | -2323.3 | $<10^{-5}$ | | | -22.77 | $<10^{-5}$ | | $10.1 \pm .03$ |

σ = standard deviation of an observation of unit weight

t-t = significance level derived by Student's t-test.

TM - Reference 12

a standard deviation, derived from σ [B(1)]

b standard deviation, derived from σ [B(2)]

TT - Reference 11

number in the original reference. As an indication of the fit of the data to a particular model we have listed $\sigma$, an estimate of the standard deviation for an observation of unit weight. This is derived, as usual, from the deviations of the data points from the fitted curve. We have used Students t-test to establish if a polynomial coefficient determined by least squares analysis differs significantly from zero. When the probability of accounting for the magnitude of a particular coefficient through random error amounts to more than 1%, that coefficient will not be considered significant.

It appears from Table I that the standard deviations, and therefore the fit of the experimental data by the two models, are roughly comparable. The charge exchange expression, in the form of a second order polynomial, seems to have a slight advantage; this is most pronounced for set TT7, on evaporation of (110) kink atoms. The image potential model for ions with charge n = 2 does almost as well; the fit with n = 3 is consistently poorer. In making this comparison it is important to realize that in the charge exchange model the data are fitted using three adjustable parameters, whereas in the image model only two are available. However, sets TM and TT9 cannot be adequately represented by a 2nd order polynomial, and the coefficients derived from the charge exchange model are not statistically significant when examined by Students t-test.

The question arises whether other functional representations of the rate might not more adequately account for the experiments. The most natural extension is to include higher order polarization effects. This is accomplished by adding a term $-\frac{1}{24}\frac{\gamma F^4}{kT}$ on the right hand side of both Eqs. (7) and (8). The results of such analysis are summarized in Table II. From this

Table II

FOURTH ORDER ANALYSIS OF FIELD EVAPORATION

| Atom | Ref. | Model | n | σ | Polynomial Coefficients B(0) | t-t | B(1) | t-t | B(2) | t-t | B(4) | t-t | $x_c$ Å | $\alpha \cdot 10^{24}$ esu | $\gamma \cdot 10^{36}$ esu |
|---|---|---|---|---|---|---|---|---|---|---|---|---|---|---|---|
| Kink | TM | Charge X | 2 | .78 | 7789 | .15 | -3503 | .14 | 441.9 | .14 | -2.06 | .13 | -27±18[a] | -195±125[b] | 98.3±61.4[c] |
| | | | 3 | | | | | | | | | | -18±12 | | |
| | | Image | 2 | .81 | -1290.0 | $<10^{-5}$ | | | -12.60 | $6.10^{-5}$ | $2.58 \cdot 10^{-2}$ | .45 | | 5.57±1.07 | -1.2±1.6 |
| | | | 3 | .82 | -2235.2 | $<10^{-5}$ | | | -29.79 | $<10^{-5}$ | .1260 | $1 \cdot 10^{-3}$ | | 13.2±1.1 | -6.01±1.59 |
| | TT7 | Charge X | 2 | .04 | 790 | .38 | -403 | .34 | 55.9 | .31 | -.297 | .26 | -3.09±1.82 | -24.7±12.9 | 14.2±6.2 |
| | | | 3 | | | | | | | | | | -2.06±1.2 | | |
| | | Image | 2 | .08 | -1260.8 | $3 \cdot 10^{-5}$ | | | -14.02 | $7 \cdot 10^{-4}$ | $4.23 \cdot 10^{-2}$ | $1.4 \cdot 10^{-2}$ | | 6.20±.16 | -2.0±2.4 |
| | | | 3 | .11 | -2208.5 | $2 \cdot 10^{-5}$ | | | -31.06 | $2 \cdot 10^{-4}$ | .140 | $2 \cdot 10^{-3}$ | | 13.7±.2 | -6.69±.31 |
| Adatom on (110) | TT9 | Charge X | 2 | .92 | 6519 | $2 \cdot 10^{-4}$ | -3048 | $2 \cdot 10^{-4}$ | 399.7 | $2 \cdot 10^{-4}$ | -2.02 | $2 \cdot 10^{-4}$ | -23.4±5.7 | -177±42 | 96.1±23.0 |
| | | | 3 | | | | | | | | | | -15.6±3.8 | | |
| | | Image | 2 | 1.13 | -1157.9 | $<10^{-5}$ | | | -19.43 | $<10^{-5}$ | .115 | $9 \cdot 10^{-5}$ | | 8.59±.77 | -5.49±1.25 |
| | | | 3 | 1.16 | -2079.3 | $<10^{-5}$ | | | -37.98 | $<10^{-5}$ | .235 | $<10^{-5}$ | | 16.8±.8 | -11.2±1.3 |
| | TT10 | Charge X | 2 | .84 | 913 | .72 | -485 | .69 | 71 | .66 | -.42 | .61 | -3.7±9.2 | -31±70 | 20±39 |
| | | | 3 | | | | | | | | | | -2.5±6.2 | | |
| | | Image | 2 | .84 | -1212.3 | $<10^{-5}$ | | | -16.05 | $<10^{-5}$ | $6.4 \cdot 10^{-2}$ | $2.6 \cdot 10^{-2}$ | | 7.09±.80 | -3.05±1.33 |
| | | | 3 | .84 | -2127.7 | $<10^{-5}$ | | | -34.97 | $<10^{-5}$ | .189 | $<10^{-5}$ | | 15.5±.8 | -9.03±1.33 |

σ = standard deviation of an observation of unit weight

t-t = significance level derived by Student's t-test

TM - Reference 12; TT - Reference 11

a standard deviation, derived from σ [B(1)]

b standard deviation, derived from σ [B(2)]

c standard deviation, derived from σ [B(4)]

it is clear that higher polarizability terms generally cause only minor changes in the standard deviation. The one exception is set TT7, for which the image potential model is remarkably improved in its ability to represent the evaporation of atoms from kink sites. It is striking, however, that only in set TT9 are all the coefficients derived by including 4th order field terms statistically significant. The improvement in $\sigma$ is therefore not always an indicator of an improved fit of the data.

An attempt has also been made to fit the experiments with a relation of the form

$$\log k_E = B(0) + B(1/2)F^{1/2} + B(2)F^2.$$

This is just the image model, without a quantitative specification of the coefficient of $F^{1/2}$. The standard deviation $\sigma$, as well as the significance levels of the coefficients, are found to be much the same as for the 2nd order polynomial curve, listed in Table I. The differences in the fit achieved by Eqs. (7) and (8) are therefore due to the different number of adjustable parameters in the two relations, and not to differences in the functional dependence on the field.

## Physical Interpretation

For regression curves involving powers of the field no higher than the second, the charge exchange model gives a smaller standard deviation than the image potential model in most of the experiments. However, this is accomplished using three parameters, and the coefficients so derived are not significant for half the data sets. The representation of the data using

the image model does not suffer from this defect and this model is therefore superior.

The addition of fourth power field terms generally lowers the standard deviation of an observation. For the charge exchange model, however, the coefficients so derived are (with the exception of set TT9) not statistically significant. The polarizabilities are negative and much too large in magnitude. The same difficulty is apparent for $x_c$, the distance of the crossing point from the image plane (allowing for penetration effects). Distances on the order of a fraction of a lattice spacing can be expected. Instead, negative values are found, placing the evaporating ions well inside the metal. The charge exchange model with inclusion of hyperpolarizability terms can therefore be rejected.

Changes in the physical parameters of the image potential model caused by fourth power field terms are less severe. In three of the data sets the additional coefficient B(4) is not statistically significant for ions with $n = 2$. Most interesting, however, is the fact that the hyperpolarizability term $\gamma$ derived for the image model from B(4) is negative for all the experiments. Its effect is therefore to counterbalance the larger values of the polarizability derived from this particular regression model. The reversal in sign from polarizability to hyperpolarizability is contrary to what is known about these quantities for simple molecules,[20] and casts added doubt upon the significance of this approach. The inclusion of terms beyond the second power in F is therefore not justified for either of the two models of field evaporation.

The image potential model, including only second order field effects, emerges as the best representation of the available experiments. It

must be emphasized again that the superiority of this model lies in the small number of parameters used to fit the data. Given the scatter in the experiments, fits achieved using three or more parameters (as in the charge exchange model) just are not consistently significant.

When a significant representation of the data is possible with both models, as it is in set TT10 for the evaporation of atoms from the (110), the differences in the two regression curves are minor. This is apparent in Fig. 3--the charge exchange representation of the experiment lies within the 95% confidence limits of the image potential curve over almost the entire range of fields.

Still to be settled is n, the ionic charge, which enters as a parameter in the image potential model of field evaporation. From the summary in Table I it is clear that all the data sets are more adequately represented by the image model with doubly charged, rather than triply charged ions. Doubly charged ions consistently give lower values of $\sigma$, the standard deviation of an observation. The image potential model with $n = +2$ is therefore the best overall choice to account for the experimental information presently available.

In view of this it is of interest to examine the polarizabilities derived for this model of field evaporation. Most striking are the really minor differences in the polarizability of atoms evaporating from kink sites, and of adatoms evaporating from sites on top of the (110). The geometry of these sites is as different as can be achieved on the surface of a bcc crystal. Despite that, the polarization term $\alpha$ is only 10% smaller for kink atoms than for the much more exposed atoms on the (110). This is a real

effect: Welch's test[19] indicates a probability less than $10^{-4}$ of accounting for the difference in $\alpha$ by random error.

It is important to note that the close agreement of the polarizability for atoms on different sites is not specific to a particular model. Polarizabilities derived from the charge exchange model are uncertain, and endowed with a large error. However, within the scatter of the data the polarizabilities on different sites are the same in this model.

## SUMMARY

Experiments on the field evaporation of tungsten atoms at kink sites, as well as adatoms on the (110) plane, can be most adequately represented by the image potential model, in which the limiting step is viewed as the escape of an ion of charge n = +2 over a Schottky saddle. Only this model gives concordant values of the effective polarizability $\alpha = \alpha_o - \alpha_+$. The polarizability is surprisingly insensitive to the location of the evaporating atom on the surface. For tungsten adatoms at a kink site $\alpha$ is $4.80 \pm .03$ Å$^3$; for atoms on the densest plane of the tungsten lattice, the (110), the polarizability is just slightly higher, with $\alpha$ at $5.24 \pm .04$ Å$^3$. This is a most helpful result: the correction for polarization energy has in the past been a major obstacle in the quantitative application of field desorption to measurements of the binding energy of atoms at a crystal surface.[21] From the rates of field evaporation it appears that the polarization correction is large: at a kink site of tungsten it amounts to 6.2 eV, which is comparable to the heat of vaporization itself. However, our analysis shows that we will incur an error of only 0.2 eV by assuming a constant polarizability for atoms at the surface, independent of their location.

It must be emphasized that this analysis should not be taken to prove the validity of the image potential model. To this end it would be necessary to know the ionic desorption energy $\chi_o^{+n}$, values of which are not available for tungsten. This would permit a comparison of the absolute rates determined in experiments with the values predicted by the image potential model. The image potential model does, however, provide the most satisfactory representation of all the data on the field dependence of evaporation.

Acknowledgements

This study was greatly helped by Dr. D. G. Brandon, Technion, and Dr. T. T. Tsong, Pennsylvania State University, who furnished us with original data. We have also benefited from discussions with R. S. Chambers and G. Ayrault.

References

1. G. Ehrlich and C. F. Kirk, J. Chem. Phys. 48, 1465 (1968).
2. E. W. Plummer and T. N. Rhodin, J. Chem. Phys. 49, 3479 (1968).
3. E. W. Müller and T. T. Tsong, Field Ion Microscopy (American Elsevier Publishing Co., New York 1969).
4. E. W. Müller, Phys. Rev. 102, 618 (1956).
5. D. M. Newns, Phys. Rev. B1, 3304 (1970).
6. D. E. Beck and V. Celli, Phys. Rev. B2, 2955 (1970).
7. R. Gomer and L. W. Swanson, J. Chem. Phys. 38, 1613 (1963).
8. G. Ehrlich, in Interatomic Potentials and Simulation of Lattice Defects, edited by J. R. Beeler, P. C. Gehlen, and R. I. Jaffee (Plenum Publishing Co., New York 1972).
9. D. McKinstry, Surface Sci. 29, 37 (1972).
10. D. G. Brandon, Brit. J. Appl. Phys. 14, 474 (1963).

11. T. T. Tsong, J. Chem. Phys. 54, 4205 (1971).

12. T. T. Tsong and E. W. Müller, Phys. Status Solidi (a)1, 513 (1970).

13. C. E. Moore, Ionization Potentials and Ionization Limits Derived from the Analyses of Optical Spectra, Nat. Stand. Ref. Data Ser., Nat. Bur. Stand. (U.S.) 34 (Sept. 1970).

14. D. G. Brandon, Phil. Mag. 14, 474 (1960).

15. D. G. Brandon, Surface Sci. 3, 1 (1965).

16. E. W. Müller, Adv. in Electronics and Electron Phys. 13, 83 (1960).

17. D. F. Barofsky and E. W. Müller, Surface Sci. 10, 177 (1968).

18. E. W. Müller, in Structure et Propriétés des Surfaces des Solides, Coll. Internat'l CNRS No. 187 (Editions CNRS, Paris 1970), p. 81.

19. For details of the statistical analyses and tests of significance, see P.G. Guest, Numerical Methods of Curve Fitting (Cambridge University Press, Cambridge 1961).

20. A. D. Buckingham and B. J. Orr, Quart. Rev. (London) 21, 195 (1967).

21. E. W. Müller, in Molecular Processes on Solid Surfaces, edited by E. Drauglis, R. D. Gretz, and R. I. Jaffee (McGraw-Hill, New York 1969), p. 400.

Security Classification

**DOCUMENT CONTROL DATA - R & D**

*(Security classification of title, body of abstract and indexing annotation must be entered when the overall report is classified)*


1. ORIGINATING ACTIVITY *(Corporate author)*

Coordinated Science Laboratory
University of Illinois
Urbana, Illinois, 61801


2a. REPORT SECURITY CLASSIFICATION

UNCLASSIFIED

2b. GROUP

3. REPORT TITLE

FIELD EVAPORATION: MODEL AND EXPERIMENT

4. DESCRIPTIVE NOTES *(Type of report and inclusive dates)*


5. AUTHOR(S) *(First name, middle initial, last name)*

Marian Vesely and Gert Ehrlich



6. REPORT DATE: June, 1972

7a. TOTAL NO. OF PAGES: 20

7b. NO. OF REFS: 21

8a. CONTRACT OR GRANT NO.: AFOSR 69-1671; AFOSR 72-2210

b. PROJECT NO.:

c.

d.

9a. ORIGINATOR'S REPORT NUMBER(S): R-568

9b. OTHER REPORT NO(S) *(Any other numbers that may be assigned this report)*: UILU-ENG 72-2229


10. DISTRIBUTION STATEMENT

This document has been approved for public release and sale; its distribution is unlimited.

11. SUPPLEMENTARY NOTES

12. SPONSORING MILITARY ACTIVITY

Air Force Office of Scientific Research, Arlington, Virginia

13. ABSTRACT


The ability of the image potential and charge exchange models to describe the evaporation of metals in a high electric field is examined. At present only the field dependence of the evaporation rate can be compared with the predictions of the two models. An analysis of the available experiments on the evaporation of tungsten atoms from kink sites, as well as from sites on top of the (110), suggests that the image potential model gives the most satisfactory representation of the data. The difference $\alpha$ between the polarizability of a neutral surface atom and an ion, which is obtained from a least-squares analysis, is found to differ little from one site to the next. For tungsten at a kink site $\alpha = 4.80 \pm .03$ Å$^3$; for an adatom on the (110), $\alpha = 5.24 \pm .04$ Å$^3$.


DD FORM 1 NOV 65 1473

Security Classification

| 14 KEY WORDS | LINK A | | LINK B | | LINK C | |
|---|---|---|---|---|---|---|
| | ROLE | WT | ROLE | WT | ROLE | WT |
| Field evaporation | | | | | | |
| Polarizability | | | | | | |